JPET Fast Forward. Published on December 18, 2006 as DOI: 10.1124/jpet.106.113639

JPET #113639

PI-3K is a critical mediator of interferon-γ-induced increases in enteric epithelial permeability

Derek M. McKay, James L. Watson, Arthur Wang, Jackie Caldwell, David Prescott, Peter M. J. Ceponis, Vincenza Di Leo and Jun Lu

Intestinal Disease Research Programme (DMM, JLW, AW, JC, DP, PMJC, JL), Department of Pathology and Molecular Medicine, McMaster University, Hamilton, Ontario, Canada

Dept. Surgical and Gastroenterological Sciences (VDL), University Hospital Padova, Italy

Running title: IFNγ and epithelial permeability

*Address Correspondence to:

Dr. Derek M. McKay
Gastrointestinal Research Group
Department of Physiology and Biophysics, 1877 HSc,
University of Calgary,
3330 Hospital Drive NW,
Calgary, Alberta T2N 4N1
Tel: (403) 220-7362
Fax: (403) 210-8999
email: dmckay@ucalgary.ca

Number of text pages: 17
Number of tables: 2
Number of figures: 12
Number of references: 43
Abstract word count: 242
Introduction word count 622
Discussion word count: 1483

Abbreviations: bisindolylmalemide I, BIM; HRP, horseradish peroxidase; IFN, interferon; NO, nitric oxide; NOS, nitric oxide synthase; ZO-1, zona occludens-1

Recommended Section Assignment – gastrointestinal, hepatic, pulmonary, and renal

Abstract

The epithelial lining of mucosal surfaces acts as a barrier to regulate the entry of antigen and pathogens. Nowhere is this function of the contiguous epithelium more important than in the gut which is continually exposed to a huge antigenic load and, in the colon, an immense commensal microbiota. We assessed the intracellular signalling events that underlie interferon-γ (IFNγ)-induced increases in epithelial permeability using monolayers of the human colonic T84 epithelial cell line. Confluent epithelial monolayers on semi-permeable supports were treated with IFNγ (20ng/ml), and barrier function assessed 48h later by measuring transepithelial electrical resistance (TER: reflects passive ion flux), fluxes of ^{51}Cr-EDTA and horseradish peroxidase (HRP), and transcytosis of non-invasive, non-pathogenic *Escherichia coli* (strain HB101). Exposure to IFNγ decreased barrier function as assessed by all 4 markers. The PI-3K inhibitors, LY294002 and wortmannin, did not affect baseline permeability characteristics, but completely blocked the drop in TER and increased fluxes of ^{51}Cr-EDTA and HRP, and significantly reduced *E. coli* transcytosis evoked by IFNγ. Also, use of the pan-PKC inhibitor, bisindolylmalemide I (5μM), but not rottlerin (blocks PKCδ), partially ameliorated the drop in TER and inhibited increased *E. coli* transcytosis. Addition of the PI-3K and PKC inhibitors to epithelia 6h after IFNγ exposure still prevented the increase in paracellular permeability, but not *E. coli* transcytosis. Thus IFNγ-induced increases in epithelial paracellular and transcellular permeability are critically dependent on PI-3K activity, which may represent an epithelial-specific target to treat immune-mediated loss of barrier function.

Polarized epithelia serve the general function of separating two biological compartments containing different contents. The epithelial lining of the intestine is bombarded with foodstuffs (i.e. dietary antigen) that are essential for the host's nutritional requirements, and is constantly exposed to a diverse community of commensal bacteria and products thereof. Thus, while epithelia lining mucosal surfaces such as the airways and reproductive tracts must exclude the entry of microbes and pathogens into the underlying mucosa, the enteric epithelium has the paradoxical challenge of fulfilling this barrier function and simultaneously digesting and absorbing nutrients. The barrier function of the epithelium is the sum of several physiological processes, including the synthesis and release of mucus from goblet cells, transcytosis of dimeric secretory IgA, lumenally-directed water movement, and the physical integrity of the epithelial layer itself (Clayburgh, et al., 2004).

With respect to gut homeostasis and mucosal immunity, it is critical that the epithelium limits the access of potentially dangerous antigen and microbes into the mucosa, and as such it is not surprising that enteric disease is often accompanied by increased gut permeability (Söderholm, et al., 2002). Under normal circumstances, lumen-derived material crosses the epithelium by either transcellular or paracellular routes: involving transit across both apical and basolateral membranes via host endocytic/exocytic processes (or active pathogen invasion), or permeation of the intercellular tight junction protein complexes, respectively. The epithelial barrier is not static, but regulated by exogenous stimuli (e.g. bacterial toxins) (Philpott, et al., 1996) and endogenous factors (e.g. cytokines) (Prasad, et al., 2005): numerous examples of cytokine regulation of epithelial paracellular permeability and tight junction structure/function have accumulated. For instance, exposure of monolayers of human colon-derived epithelial cell lines to interferon-γ (IFNγ) (± other cytokines, such as tumour necrosis factor-α (TNFα)) results in a significant increase in monolayer permeability (Madara and Stafford, 1989; Ivanov, et al.,

2004; Watson, et al., 2004; Wang, et al., 2005). Although less extensive, *in vivo* studies have implicated IFNγ in increased gut permeability evoked by stress and inflammation, corroborating the *in vitro* analyses (Cenac, et al., 2004; Yang, et al., 2002)

IFNγ production is increased in a variety of diseases and given its' ability to affect epithelial integrity, we, and others, have pursued the mechanism by which IFNγ leads to increased epithelial permeability, with the goal of elucidating a specific target that when antagonized prevents this effect of IFNγ, maintaining the barrier property of the epithelium. Since the original observations of IFNγ-induced increases in epithelial function (Madara and Stafford, 1989), it has become clear that this is not due to the induction of apoptosis (Bruewer, et al., 2003), but instead is associated with rearrangement of the actin cytoskeleton and internalization and reduced expression of tight junction proteins (Utech, et al., 2005; Youakim and Ahdieh, 1999). However, less is known of events that transduce IFNγ-IFNγ receptor interaction into the physiological outcome of increased epithelial permeability, an event that takes 24-48 hours to manifest and is dependent on protein synthesis. Moreover, there is a dearth of data on IFNγ effects on transcellular permeability, which has recently been presented as a portal of entry for bacteria into the gut mucosa (Clark, et al., 2005; Nazli, et al., 2004).

Recently we showed that pharmacological blockade of IFNγ-induced signal transducer and activator of transcription (STAT)-1 activation did not prevent the IFNγ-induced reduction in transepithelial electrical resistance (an index of paracellular permeability) (Watson, et al., 2004). Extending these observations, we present data in support of phosphatidylinositol 3' kinase (PI-3K) and protein kinase C (PKC) as mediators of IFNγ-induced increases in epithelial paracellular permeability and the transcytosis of non-invasive, non-pathogenic *Escherichia coli* across monolayers of human gut-derived epithelial cells.

METHODS

Cell Culture and Reagents

The human colon-derived T84 epithelial cell line was cultured at 37°C with 5% CO_2 in a 1:1 mixture of Dulbecco's modified Eagle's medium (DMEM) and Ham's F-12 medium supplemented with 2% (v/v) penicillin-streptomycin and 1.5% (v/v) HEPES (all from Invitrogen, Burlington, ON) and 10% fetal bovine serum (CanSera, Toronto, ON). Human recombinant IFNγ and interleukin (IL)-4 were from R&D Systems (Minneapolis, MN). The following reagents were purchased from Sigma Chemical Co. (St. Louis, MO): LY294002 and wortmannin (both inhibit PI-3K), -(-) epigallocatechin gallate (EGCG: green tea poly-phenol that inhibits STAT1 phopshorylation), L-NAME (N^{ω}-nitro-L-arginine methyl ester: inhibits nitric oxide synthase (NOS)) and bisindolylmalemide I (BIM: inhibitor of PKC isoforms). The phosphatidylinositol analogue (PI; 1L-6-hyrdomethyl-chiro-iniositol 2-[(R)-2-O-methyl-3-O-octadecylcarbonate]; blocks PH domain protein interactions), AKT-inhibitors II (SH-5 and API-2 (triciribine)), rottlerin (blocks PKCδ), L-NMMA (N^{G}-monomethyl-L-arginine: inhibits NOS), and L-NIL (N^{6}-(1-iminoethyl)-lysine HCl): inhibits inducible NOS) were from Calbiochem (San Diego, CA). Enteropathogenic *Escherichia coli* (EPEC) and the non-pathogenic *E. coli* strain HB101 were provided by Dr. P.M. Sherman (University of Toronto, Toronto, ON) and were cultured in Luria Bertani broth (LB) and on LB agar plates. Transformed *E. coli* HB101 harbouring a prokaryotic enhanced green fluorescent protein (eGFP) expression vector (Clontech, Mountain View, CA) were maintained by culture in ampicillin (100μg/ml; Sigma). The concentrations of cytokines, bacteria and pharmacological agents used are based on related studies and are specified in the figure legends. Cytokines and drugs were added into the basal compartment of the culture well as a 45-60 min pre-treatment (unless otherwise stated), while the

E. coli were applied to the apical surface of the epithelial monolayer to mimic appropriate routes of *in vivo* exposure.

Assessment of Epithelial Barrier function

1) Transepithelial Electrical Resistance (TER)

T84 cells ($1x10^6$) were seeded onto $1cm^2$ semi-permeable filter supports (pore size 0.4 or 3.0μm; Costar, Corning Inc., Cornell, NY), and cultured for ~7days until the TER of the monolayer ≥ $1000\Omega \cdot cm^2$ as measured by a voltmeter and companion electrodes (Millipore, Bedford, MA). TER of each monolayer was measured before and after treatment and is expressed as the percentage of pre-treatment TER values to normalize for variation in absolute values between individual monolayers (Watson, et al., 2004).

2) Flux of marker molecules

After the final TER reading 5μCi of the paracellular permeability probe ^{51}Cr-EDTA (mw ~360Da; Sigma Chemical Co.) were added to the apical compartment of filter-grown T84 cell monolayers and 4h later duplicate 0.5ml samples were retrieved from the basal compartment and radioactivity determined in a γ-counter. Results are expressed as counts per minute (CPM). In additional epithelial preparations, the mucosal-to-serosal flux of horseradish peroxidase (HRP: type VI mw. ~ 44 KDa: Sigma Chemical Co.) was assessed as a marker of transcellular transport. Briefly, 10μM HRP was added to the lumenal side of the epithelial layer, 2h later duplicate 10μl aliquots of the basolateral culture media were mixed with 80μg/ml o-dianisidine (Sigma) in 100μl reaction buffer and HRP activity determined in a kinetic assay by measuring absorbance at 470nm at 30 sec intervals over a 2 min period. Results are expressed as the percentage recovery of HRP (Berin, et al., 1999).

3. Bacterial internalization and translocation

Internalization: $1x10^6$ T84 cells were cultured in 12-well plates until ~80% confluent (i.e. 3-4 days), at which time IFNγ ± pharmacological inhibitor were added to the epithelium followed by $1x10^6$ cfu *E. coli* HB101 (in log phase of their growth) 48h later. Sixteen hours later the culture medium was aspirated and replaced with fresh medium containing 250μg/ml gentamicin (Invitrogen) for 2h to kill extracellular bacteria. Epithelial preparations were rinsed (x4) with sterile PBS (37°C), lysed in 1ml cold (4°C) 0.1% Triton X-100/PBS for 15 min and the lysates re-suspended. Serial dilutions of each lysate were streaked onto LB agar plates that were incubated under aerobic conditions at 37°C for 24h and bacterial colonies subsequently counted. To complement this quantitative assessment, bacteria were visualized by immunofluorescent detection. Filter-grown T84 monolayers treated with IFNγ ± LY294002 for 48h were exposed to 10^6 cfu *E. coli* HB101-eGFP. Sixteen hours later, monolayers were rinsed (x4) with sterile PBS, fixed in 10% neutral-buffered formalin for 20 min, rinsed again and treated with rodamine-conjugated anti-*E. coli* antibodies (Sigma). Monolayers were rinsed in sterile PBS, excised from the culture well mounts and mounted on poly-l-lysine-coated microscope slides in anti-fade mounting medium (Biomedia, Foster City, CA). Collection of both *en face* and z-series images was performed with a LSM510 laser-scanning confocal microscope (Carl Zeiss, Germany) and a Windows 2000-based computer system and LSM510 v2.3 software. Because the monolayers are not permeabilized the anti-*E. coli* antibodies are excluded from the intracellular space and so internalized bacteria appear green because of eGFP expression and extracellular bacteria appear yellow/orange (i.e. eGFP + rodamine).

Translocation: T84 cells were cultured on porous filter-supports (pore size = 3.0μm) until monolayers were electrically confluent (i.e. TER>1000Ω·cm^2), treated with IFNγ ± pharmacological inhibitors and 48h later *E. coli* HB101 (10^6 cfu) were added to the apical side of

the monolayer. Sixteen hours later, 10µl of basolateral culture medium was collected, inoculated onto LB agar plates and cultured at 37°C for 24h (Nazli, et al., 2004). Colony growth was enumerated by a semi-quantitative score (0-5) reflective of a logarithmic scale: 1 = no bacterial colonies, 2 = <10 colonies, 2 = 10-100 colonies, 3 = >100 colonies but countable, 4 = >100 colonies, uncountable but individual colonies can be defined, and 5 = bacterial lawn (individual colonies cannot be distinguished).

Western Blotting

In these experiments, $2x10^6$ T84 cells/well were seeded in 6-well tissue-culture treated plates or filter supports and exposed to the various experimental treatments. Whole cell lysates were prepared by scraping cells in ice-cold RIPA buffer containing protease (Complete protease inhibitor cocktail, Roche, Indianapolis, IN) and phosphatase inhibitors (100mM NaF, 100mM $NaVO_3$ (Sigma Chemical Co.)) and allowing lysis to proceed for 20min on ice, with vigorous vortexing at 10 and 20min. Lysates were clarified by centrifugation and the supernatant collected and stored at -70°C. Protein concentration was determined using the BioRad/Bradford microplate assay (BioRad, Hercules, CA). Protein extracts (20-40µg) in reducing-loading buffer were boiled and electrophoresed through 4-10% (29:1 acrylamide/bisacrylamide) SDS gels. Separated proteins were electroblotted to Immobilon nitrocellulose membrane (Millipore), and blocked in 5% non-fat powdered milk/TBST or 5% BSA/TBST for 1h. Primary antibodies used were anti-IRF1, 1:4000 and anti-actin, 1:500 (Santa Cruz Biotechnology, Santa Cruz, CA); anti-pS_{473}-Akt, 1:1000 and anti-Akt, 1:1000 (Cell Signalling Technology, Danvers, MA), anti-PKC (α, β, γ), 1:500 (Upstate Cell Signalling Solutions, Charlottesville, VA) and anti-pan phospho-PKC, 1:500 (Cell Signalling Technology). Blots were washed and incubated with secondary antibody-HRP conjugates for 1h (goat anti-rabbit or rabbit anti-mouse (both at 1:4000; Santa

Cruz Biotech.)) then washed extensively and immunoreactive proteins visualized using enhanced chemiluminescence (ECL, Amersham Pharmacia, Piscataway, NJ) and exposing the membrane to Kodak XB-1 film (Watson, et al., 2004).

Reverse transcriptase Polymerase Chain Reaction (RT-PCR)

Total RNA was extracted from semi-confluent T84 cell layers (grown in 6 well culture plates) ± 6h of exposure to IFNγ (20 ng/ml) and RT-PCR performed using an established protocol (Watson, et al., 2004) with the following primer sequences: iNOS, forward 5'-AGCACATTCAGATCCCCAAG-3' and reverse 5'-TCCAGGATACCTTGGACCAG-3' (product size = 298 base pairs (bp)); constitutive (c)NOS, forward, 5'-CCTGACAACCCCAAGACCTA-3' and reverse 5'-CAGCCTCTGGACAGATGTGA-3' (product size = 495 bp); and β-actin as a housekeeping gene, forward 5'-CCACAGCAAGAGAGGTATCC-3' and reverse 5'-CTGTGGTGGTGAAGCTGTAG-3' (product size = 437 bp). Products were electrophoresed through a 2% agarose gel and the amplified cDNA visualized under UV light by ethidium bromide staining.

Electrophoretic Mobility Shift Assay (EMSA)

Nuclear extracts and EMSAs were conducted according to a previously published protocol (Ceponis, et al., 2000). Briefly, nuclear extracts (5-10μg protein) in binding buffer were incubated for 30 min with ^{32}P-dCTP (NEN Life Science Products, Boston, MA) labelled oligonucleotide probe (hSIE) containing a high-affinity STAT1 binding site (5'-GTCGACATTTCCCGTAAATC-3' and 5'-TCGACGATTTACGGGAAATG-3'). Samples were electrophoresed through a non-denaturing 6% (40:1 bis/acrylamide) polyacrylamide gel for 2.5h

at 120V, dried under vacuum at 80°C and visualized by autoradiography after overnight exposure (-70°C) to Kodak XAR film.

Data Analysis

Data are presented as mean ± standard error of the mean (SEM), were n is defined as the number of experiments or epithelial preparations examined. Data were compared by ANOVA followed by Newman-Keuls statistical comparisons, or by Students' paired or unpaired t-tests where appropriate. A level of statistical significant difference was accepted at $p<0.05$.

RESULTS

IFNγ-induced increases in epithelial permeability are PI-3K dependent

We, and others, have shown that IFNγ-induced decreases in TER are time-dependent and are consistently and significantly reduced at 48h post-treatment and not earlier. For instance, in a representative experiment from the current analysis monolayers exposed to IFNγ (20 ng/ml) had TER values of 116±14 (4h), 131±18 (8h), 108±16 (12h), 112±13 (24h) and 50±9% (48h) of pre-treatment values (mean ± standard deviation; 3 epithelial monolayers; numbers in parentheses indicate time post-IFNγ). Therefore we concentrated our mechanistic studies on the 48h post-IFNγ time-point.

To assess a role for PI-3K in IFNγ-induced increases in epithelial permeability, two well-characterized inhibitors of PI-3K activity, LY294002 (LY) and wortmannin, were utilized. The barrier property of epithelial cell monolayers was gauged by TER and transepithelial fluxes of ^{51}Cr-ETDA and HRP (markers of the paracellular and transcellular permeation pathways, respectively) 48h after exposure to IFNγ ± a 1h pre-treatment with LY or wortmannin. Inhibition of PI-3K activity significantly reduced, or prevented, the increase in epithelial permeability evoked by IFNγ exposure, as assessed by each marker of barrier function (Figure 1). Corroborating these observations, use of a phosphatidylinositiol analogue that inhibits the binding of PH domain-containing proteins to PI-3K (e.g. phosphoinositide-dependent kinase-1 (PDK1)) also prevented the drop in T84 monolayer TER caused by IFNγ (Figure 2). Moreover, addition of LY into the culture well 3 or 6h after IFNγ still prevented the drop in TER evoked by this cytokine (Figure 3). In contrast, the drop in TER caused by infection with enteropathogenic *E. coli* (EPEC) was unaffected by LY co-treatment (Figure 4), indicating stimulus specificity in the control of epithelial barrier function.

It has been suggested that the IFNγ effect on epithelial barrier function is due to the induction and liberation of nitric oxide (NO) (Unno, et al., 1997) although others have disputed this (Satake, et al., 2001). RT-PCR analysis revealed that IFNγ treatment evokes small increases in constitutive (c)-NOS mRNA and significant increases in inducible (i)-NOS mRNA in T84 epithelial cells (Figure 5 inset), and while some debate exists relating to NO production by these cells, others have shown that they can express iNOS mRNA and protein (Kiang, et al., 2003; Hamalainen, et al., 2002). Despite this, the use of L-NAME and L-NMMA, two agents that block all isoforms of NOS, and L-NIL, an inhibitor that targets iNOS, all failed to ameliorate IFNγ-evoked reductions in TER (Figure 5).

We have shown that IFNγ treatment activates STAT1 in enteric epithelia (McKay, et al., 2000) and PI-3K activation by IFNγ in various cell lines has been reported (Choudhury, 2004; Hwang, et al., 2004) In addition, PI-3K has been implicated in phosphorylation of STAT1 ^{727}serine, which may be key for maximal transcriptional activity. Therefore, addressing the issue of PI-3K regulation of STAT1 function, T84 cells were treated with IFNγ ± LY and STAT1 activation assessed by DNA-binding on EMSA, ^{727}serine phosphorylation levels on western blots and transcription of interferon regulated factor (IRF)-1 (a STAT1-dependent gene). Neither LY nor wortmannin affected IFNγ-induced STAT1 DNA binding, ^{727}serine phosphorylation (wortmannin data not shown) or IRF-1 protein expression (Figure 6), whereas known inhibitors of STAT1 activation, namely epigallocatechin gallate (EGCG) and aurintricarboxylic acid (ATA) (Watson, et al., 2004), did reduce IFNγ-stimulated STAT1 phosphorylation, DNA-binding and transcriptional activity (Figure 6). These findings support the postulate that IFNγ-induced increases in epithelial permeability are dependent on mobilization of PI-3K and are unlikely to be due to PI-3K interference with STAT1 activity.

The PI-3K target AKT is not involved in IFNγ-induced increases in epithelial permeability

AKT is phosphorylated and activated by PDK1 in response to generation of plasma membrane phosphatidylinositol-3,4,5-trisphosphate ($PI(3,4,5)P_3$) and $PI(3,4)P_2$ by Class I PI-3K. AKT activation is a major downstream effector molecule following PI-3K activation and so we assessed a role for this kinase in the IFNγ-induced, PI-3K-dependent T84 cell barrier dysfunction. Pharmacological interference with AKT activation via SH-5 or API-2 failed to alleviate the drop in TER caused by IFNγ (Figure 7A). Corroborating these functional studies, immunoblotting of whole cell protein extracts from IFNγ-treated (50-200ng/ml; 10 min to 24h) epithelia did not reveal any consistent evidence in support of AKT activation as defined by phosphorylation of AKT ^{473}serine (Figure 7B (data for 6, 8 and 24h not shown)). These data suggest that activation of AKT, perhaps constitutive in T84 cells (see control lane on Figure 7B), is not enhanced by IFNγ treatment and is not required for the disruption of barrier function.

Inhibition of PKC isoforms ablates IFNγ induced, but not IL-4-induced, increases in epithelial paracellular permeability

PKC has been implicated as a mediator of IFNγ-driven events (Deb, et al., 2003; Ivaska, et al., 2003) and in the control of epithelial paracellular permeability (Weiler, et al., 2005; Song, et al., 2001). As shown in Figure 8A, addition of the pan-PKC inhibitor bisindolylmalemide I (BIM; 5μM) to T84 epithelial cell monolayers prior to IFNγ significantly reduced the subsequent drop in TER (200nM BIM did not ameliorate IFNγ-induced reductions in T84 monolayer TER). Moreover, addition of BIM to epithelial monolayers 6h after IFNγ also resulted in a significant inhibition of the IFNγ effect, and indeed the magnitude of the preservation of epithelial barrier function was virtually identical to that observed when the PKC inhibitor was used in a 45 min

treatment protocol (Figure 8B). However, in contrast to PI-3K inhibition, the effect of PKC inhibition resulted in only partial maintenance of epithelial paracellular permeability in the face of IFNγ challenge (Figure 8A). Moreover, when LY294002 and BIM were used in combination, there was total preservation of epithelial TER following exposure to IFNγ (Figure 9) and this is in agreement with the effect of PI-3K inhibition alone (Figure 1). These data suggest that PI-3K is upstream of PKC in the mediation of IFNγ effects on TER (a measure of paracellular permeability), or if the pathways are in parallel, then the small effect of PKC-inhibition is masked by simultaneous blockade of PI-3K activity. In addition, we should consider the possibility that BIM may not elicit a complete pharmacological blockade of PKC (noting that TER is measured 48h after addition of the inhibitor) or that PI-3K mobilizes other signals that add to or synergise with PKC to cause the drop in TER.

Rottlerin (5μM) affected neither the IFNγ-evoked decreases in TER nor the increased bacterial transcytosis (n=7-16 epithelial monolayers from 3 experiments; data not shown). Based on the selectivity of this drug, it appears that PKCδ is not the PKC isofrom participating in IFNγ-induced increases in epithelial permeability

Furthermore, BIM pre-treatment did not affect the drop in TER observed 24h after treatment with IL-4, with the higher dose of the PKC-inhibitor (i.e. 5μM) actually enhancing the drop in TER evoked by IL-4 (Table 1).

Analysis of whole cell protein extracts from IFNγ (± LY)-treated filter-grown epithelia failed to reveal any consistent increase in PKC phosphorylation at 15-60 min or 7h post-treatment using an antibody that detects phosphorylated PKCα, βI, βII and δ (n=3: data not shown).

IFNγ enhances internalization of commensal bacteria and transcytosis across the epithelium via PI-3K and PKC-dependent mechanisms

The observation of IFNγ-induced increased transepithelial flux of HRP led us to posit that exposure to IFNγ could result in increased apical-to-basal transit of *E. coli* strain HB101; again focusing on the 48h time-point. In 4 separate experiments, T84 epithelial cells exposed to IFNγ had increased numbers of intracellular bacteria, since they could be cultured after gentamicin treatment that would kill extracellular organisms (Table 2). This was confirmed by immunolocalization studies (Figure 10A). The increased bacterial internalization translated into increased transcytosis across IFNγ treated epithelia. Pre-treatment with LY294002 significantly reduced bacterial internalization (Figure 9A, Table 2) and transcytosis was inhibited by pre-treating the T84 epithelial cell monolayers with either LY294002 or BIM (Figure 9B-D). However, and in contrast to the TER, inhibition of PI-3K and PKC activity were equally effective in reducing IFNγ-induced bacterial transcytosis. Indeed, in 9 separate experiments utilizing 39 epithelial monolayers, not a single grade 5 was assigned to the bacterial translocation in IFNγ+BIM treated epithelia (Figures 10 & 11), suggesting that PKC has a more prominent role in the control of transcellular permeability/bacterial transcytosis compared to the regulation of the paracellular permeation pathway (Figure 11). Moreover, addition of LY294002 or BIM to epithelial monolayers 6h after IFNγ did not prevent the IFNγ-evoked epithelial transcytosis of *E. coli* HB101 (data not shown).

DISCUSSION

Maintenance of the enteric epithelial barrier is important in digestive health, functioning to retard the movement of antigens and bacteria from the gut lumen into the mucosa. Indeed, increased epithelial permeability is associated with infectious and idiopathic enteropathies, including Crohn's disease (Söderholm, et al., 2002; Lindberg, et al., 1995) Inappropriate/excessive increases in epithelial permeability would be expected to promote or prolong enteric inflammation, while controlled increases could be beneficial, easing the passage of phagocytes and complement into the lumen of the gut. Studies with epithelial cell lines and mice reveal that IFNγ, which can be released in controlled immune responses or as a component of pathophysiological reactions, decreases epithelial barrier function (Cenac, et al., 2004; Clark, et al., 2005;). Elegant studies have documented changes in epithelial tight junction protein (e.g. claudins, occludin, ZO-1) expression and localization following IFNγ exposure (± TNFα co-treatment) (Prasad, et al., 2005; Utech, et al., 2005; Wang, et al., 2005). Thus the goal of this study was to identify intracellular signalling pathways that convert IFNγ-IFNγ receptor interaction into decreased barrier function.

IFNγ can activate PI3K, and we implicated this enzyme in the decreases in TER caused by conditioned medium from activated immune cells (McKay, et al., 2000) which contained significant amounts of IFNγ, and in the drop in TER evoked by IL-4 (Ceponis, et al., 2000). Pharmacological inhibition of PI-3K activity blocked IFNγ-induced increases in epithelial permeability. STAT1 mobilization is a major signalling event in response to IFNγ and PI-3K and STAT1 can cross-talk (Choudhury, 2004). However, PI-3K inhibition failed to affect IFNγ-induced STAT1 activation in T84 cells as assessed by DNA binding, tyrosine phosphorylation, and transcriptional activity. These data, coupled with our previous study (Watson, et al., 2004), suggest that IFNγ regulation of epithelial paracellular permeability is not strictly STAT1-

dependent. Additionally, NO (iNOS is a STAT1-regulated gene) has been implicated (Unno, et al., 1997), and refuted (Satake, et al., 2001), as the mediator of IFNγ evoked decreases in TER across Caco-2 cell monolayers; we found that 3 different NOS inhibitors did not prevent the IFNγ-effects on T84 epithelial permeability. Thus, the current study, data on the effects of IL-4 on epithelial paracellular permeability, and IFNγ regulation of tight junction protein insertion in the cell membrane, all identify PI-3K as a crucial signalling molecule mediating cytokine-evoked increases in paracellular permeability. Yet, additional pathways regulating paracellular permeation exist since EPEC-induced reductions in TER (Figure 4) and those caused by exposure to metabolic stress and non-pathogenic *E. coli* were unaffected by inhibition of PI-3K activity (Nazli, et al., 2004). Therefore, blockade of epithelial PI-3K signalling could be a specific means to reduce immune-mediated epithelial barrier dysfunction *in vivo*.

Assessing paracellular permeability revealed that: i) AKT is not required for the PI-3K-dependent IFNγ disruption of epithelial integrity; ii) pan-inhibition of PKC significantly reduced the effects of IFNγ but to a lesser degree than PI-3K inhibition; iii) inhibitors of PI-3K and PKC added to epithelia 6h after IFNγ still ablated the effects of IFNγ on TER; and iv) inhibition of PKC pathways did not affect IL-4-evoked reductions in TER.

AKT is an important mediator of many PI-3K-dependent events, but while LY294002 completely prevented IFNγ-induced decreases in TER, inhibitors of AKT activity failed to influence the IFNγ effect. While novel, PI-3K-dependent, AKT-independent signalling is not unique: addition of IFNγ to erythroid progenitors resulted in a PI-3K sensitive induction of Bcl-x expression while AKT phosphorylation remained unaltered (Paiboonsukwong, et al., 2003). While we have no evidence in support of ATK involvement in the IFNγ disruption of epithelial integrity, inhibition of AKT activity is beneficial in preventing deceases in barrier function

where apoptosis is involved (Ginzberg, et al., 2004): apoptosis does not play a prominent role in IFNγ evoked increases in epithelial permeability (Bruewer, et al., 2003;Watson, et al., 2004).

Protein kinase C can be activated in response to IFNγ (Deb, et al., 2003; Ivaska, et al., 2003), and BIM consistently reduced IFNγ-evoked reductions in TER. This finding is in accordance with PKC-regulation of epithelial barrier formation and maintenance, where, to-date, the α, ε, δ, θ and ζ isoforms of PKC have been implicated (Banan, et al., 2005; Tomson, et al., 2004; Weiler, et al., 2005). Immunoblotting did not show increased PKCα, β or δ phosphorylation 15-60 min or 7h post-IFNγ treatment. The latter is consistent with the pharmacological data (i.e. rottlerin experiments), but one would have predicted PKCα or PKCβ activation, since BIM blocks these isoforms. However, PKC activation could occur at intermediate time points (2-6h; see below), and indeed IFNγ can elicit multi-phasic PKC activation (Mattila, et al., 1993). In addition, the LY294003+BIM treatment, like exposure to LY294002 alone, resulted in complete ablation of the ability of IFNγ to reduce TER. This suggests that either PI-3K is upstream of PKC or, if the pathways are distinct, that the smaller effect of PKC inhibition is overwhelmed by blocking PI-3K. Clearly, PI-3K-dependent and PKC-independent control of epithelial paracellular permeability occurs since LY294002 prevents IL-4-induced reductions in TER (Ceponis, et al., 2000), while BIM does not (Table 1). Finally, a MAPK cascade is activated in response to IFNγ, but we found no involvement of either Erk 1/2 or p38 MAPK in IFNγ-evoked increases in paracellular permeability (Watson, et al., 2004).

The fact that the inhibitors of PI-3K and PKC activity can be added to the epithelium up to 6h after IFNγ and still block the decreased TER is intriguing. Several hypotheses explain these findings including: 1) synthesis and release of a mediator that feeds back onto the enterocyte to activate PI-3K, 2) biphasic PI-3K and PKC activation (Marino, et al., 2003; Condliffe, et al.,

2005) or 3) a delayed receptor trans-activation event, analogous to that presented for cholinergic and EGF control of epithelial Cl^- secretion (Keely, et al., 1998). Thus, while the intricacies of IFNγ-PI-3K-PKC signalling (and parallel pathways) in the control of epithelial paracellular permeability are yet to be fully defined, there appears to be a window of opportunity in which inhibition of immune-mediated increases in epithelial permeability would be a feasible therapeutic option.

Extensive efforts have been devoted to understanding the structure and regulation of the epithelial tight junction, as this is a site of vulnerability that can be exploited by pathogens (Philpott, et al., 1996). However, non-invasive bacteria can cross the epithelium via a transcellular route. For instance, translocation of *E. coli* (strain HB101) across metabolically-stressed T84 cell monolayers was dependent on a functional cytoskeleton (Nazli, et al., 2005), IFNγ promoted the transcytosis of *E. coli* (strain C25) across monolayers of human Caco2 epithelia (Clark, et al., 2005), and TLR4 was implicated in *E. coli* (strain DH5a) internalization into the IEC-6 rat epithelial cell line (Neal, et al., 2006). *E. coli* HB101 is non-invasive and minimal translocation occurs across naïve epithelial monolayers (Philpott, et al., 1996). Here, initial assessment revealed greater numbers of *E. coli* HB101 inside IFNγ-treated T84 cells and this was complemented by semi-quantitative analyses showing a significant increase in bacterial transcytosis. This is a significant observation since *E. coli* HB101 cannot invade the enterocyte, and in the context of IBD where a component of the commensal microflora (Darfeuille-Michaud, et al., 2004) has been implicated in disease etiology. Inhibition of PI-3K or PKC significantly reduced IFNγ-driven *E. coli* HB101 internalization and transcytosis, underscoring the importance of maintaining the transcellular barrier function of the epithelium. These transcytosis studies revealed two additional noteworthy points. First, unlike TER, inhibition of PI-3K and PKC reduced IFNγ-induced bacterial transcytosis to a similar degree, implying a more prominent role

for PKC in transcellular rather than paracellular permeability in this model. Second, addition of the PI-3K and PKC inhibitors 6h after IFNγ did not significantly reduce the increased bacterial transcytosis. Thus, while PI-3K and PKC are important regulators of epithelial barrier function, their relative importance varies depending on whether paracellular or transcellular permeability is considered. This highlights the complexity, and by inference the importance, of appropriate control of the epithelium's barrier function.

In summary, exposure to IFNγ mobilizes STAT1, PI-3K, PKC and MAPKs that culminate in the regulation of up to 500 genes and significant physiological changes. Employing human T84 epithelial cells, we show that increases in epithelial permeability evoked by IFNγ are PI-3K- and PKC-dependent events (Figure 12). Moreover, and unexpectedly, inhibition of PI-3K and PKC can be delayed for up to 6h after IFNγ exposure and still result in a significant amelioration of the increased paracellular, but not transcellular, permeability. Identification of specific PI-3K and PKC isoforms that regulate epithelial permeability is a major undertaking and is the next vital step as we seek to precisely delineate cytokine control of the epithelial barrier. Similarly, additional steps leading from IFNγ-IFNγ receptor interaction to increased endocytosis and reduced expression/altered localization of tight junction proteins need to be elucidated. While many issues remain, PI-3K and PKC have been identified as crucial regulators or epithelial permeability and may represent epithelial–specific targets in the treatment of immune-mediated decreases in epithelial barrier function.

References

Banan A, Zhang LJ, Shaikh M, Fields JZ, Choudhary S, Forsyth CB, Farhadi A and Keshavarzian A (2005) Theta Isoform of protein kinase C alters barrier function in intestinal epithelium through modulation of distinct claudin isotypes: a novel mechanism for regulation of permeability. *J Pharmacol Exp Ther* **313**:962-982.

Berin MC, Yang P-C, Ciok L, Waserman S and Perdue MP (1999) Role of IL-4 in macromolecular transport across intestinal epithelium. *Am J Physiol Cell Physiol* **276**:C1046-C1052.

Bruewer M, Luegering A, Kucharzik T, Parkos CA, Madara JL, Hopkins AM and Nusrat A (2003) Proinflammatory cytokines disrupt epithelial barrier function by apoptosis-independent mechanisms. *J Immunol* **171**:6164-6172.

Cenac N, Chin AC, Garcia-Villar R, Salvador-Cartier C, Ferrier L, Vergnolle N, Buret AG, Fioramonti J and Bueno L (2004) PAR2 activation alters colonic paracellular permeability in mice via IFN-γ–dependent and -independent pathways. *J Physiol* **558**:913-925.

Ceponis PJM, Botelho F, Richards CD and McKay DM (2000) Interleukins 4 and 13 increase intestinal epithelial permeability via a phosphatidylinositol-3' kinase dependent pathway: lack of evidence for stat-6 involvement. *J Biol Chem* **275**:29132-29137.

Choudhury GG (2004) A linear signal transduction pathway involving phosphatidylinositol 3-kinase, protein kinase Cε, and MAPK in mesangial cells regulates interferon-γ-induced STAT1α transcriptional activation. *J Biol Chem* **279**:27399-27409.

Clark E, Hoare C, Tanianis-Hughes J, Carlson GL and Warhurst G (2005) Interferon-γ induces translocation of commensal *Escherichia coli* across gut epithelial cells via a lipid raft-mediated process. *Gastroenterology* **128**:1258-1267.

Clayburgh DR, Shen L and Turner JR (2004) A porous defense: the leaky epithelial barrier in intestinal disease. *Lab Invest* **84**:282-291.

Condliffe AM, Davidson K, Anderson KE, Ellson CD, Crabbe T, Okkenhaug K, Vanhaesebroeck B, Turner M, Webb L, Wymann MP, Hirsch E, Ruckle T, Camps M, Rommel C, Jackson SP, Chilvers ER, Stephens LR and Hawkins PT (2005) Sequential activation of class IB and class IA PI3K is important for the primed respiratory burst of human but not murine neutrophils. *Blood* **106**:1432-1440.

Darfeuille-Michaud A, Boudeau J, Bulois P, Neut C, Glasser AL, Barnich N, Bringer MA, Swidsinski A, Beaugerie L and Colombel JF (2004) High prevalence of adherent-invasive *Escherichia coli* associated with ileal mucosa in Crohn's disease. *Gastroenterology* **127**:412-421.

Deb DK, Sassano A, Lekmine F, Majchrzak B, Verma A, Kambhampati S, Uddin S, Rahman A, Fish EN and Platanias LC (2003) Activation of protein kinase Cδ by IFN-γ. *J Immunol* **171**:267-273.

Ginzberg HH, Shannon PT, Suzuki T, Hong O, Vachon E, Moraes T, Abreu MT, Cherepanov V, Wang X, Chow CW and Downey GP (2004) Leukocyte elastase induces epithelial apoptosis: role of mitochondrial permeability changes and Akt. *Am J Physiol Gastrointest Liver Physiol* **287**:G286-G298.

Hamalainen M, Lahti A and Moilanen E (2002) Cacineurin inhibitors, cyclosporine A and tarcolimus inhibit expression of inducible nitric oxide synthase in colon epithelial and macrophage cell lines. *Eur J Pharmacol* **448**:239-244.

Hwang SY, Jung JS, Lim SJ, Kim JY, Kim TH, Cho KH and Han IO (2004) LY294002 inhibits interferon-γ-stimulated inducible nitric oxide synthase expression in BV2 microglial cells. *Biochem Biophys Res Commun* **318**:691-697.

Ivanov AI, Nusrat A and Parkos CA (2004) Endocytosis of epithelial apical junctional proteins by a clathrin-mediated pathway into a unique storage compartment. *Mol Biol Cell* **15**:176-188.

Ivaska J, Bosca L and Parker PJ (2003) PKCε is a permissive link in integrin-dependent IFN-γ signalling that facilitates JAK phosphorylation of STAT1. *Nat Cell Biol* **5**:363-369.

Kiang JG, Warke VG and Tsokos GC (2003) NaCN-induced chemical hypoxia is associated with altered gene expression. *Mol Cell Biochem* **254**:211-216.

Keely SJ, Uribe JM and Barrett KE (1998) Carbachol stimulates transactivation of epidermal growth factor receptor and mitogen-activated protein kinase in T84 cells. Implications for carbachol-stimulated chloride secretion. *J Biol Chem* **273**:27111-27117.

Lindberg E, Soderholm J, Olaison G, Tysk C and Jarnerot G (1995) Intestinal permeability to polyethylene glycols in monozygotic twins with Crohn's disease. *Scand J Gastroenterol* **30**:780-783.

Madara JL and Stafford J (1989) Interferon-γ directly affects barrier function of cultured intestinal epithelial monolayers. *J Clin Invest* **83**:724-727.

Marino M, Acconcia F and Trentalance A (2003) Biphasic estradiol-induced AKT phosphorylation is modulated by PTEN via MAP kinase in HepG2 cells. *Mol Biol Cell* **14**:2583-2591.

Mattila P, Ustinov J and Renkonen R (1993) Interferon-γ induces a phospholipase D-dependent release of arachidonic acid from endothelial cell membranes: a mechanism for protein kinase C activation. *Scand J Immunol* **38**:197-200.

McKay DM, Botelho F, Ceponis PJ and Richards CD (2000) Superantigen immune stimulation activates epithelial STAT-1 and PI 3-K: PI 3-K regulation of permeability. *Am J Physiol Gastrointest Liver Physiol* **279**:G1094-G1103.

Nazli A, Wang A, Steen O, Prescott D, Lu J, Perdue MH, Soderholm JD, Sherman PM and McKay DM (2005) Enterocyte cytoskeleton changes are crucial for enhanced translocation of commensal bacteria across metabolically stressed gut epithelia. *Infect Immunity* **74**:192-201.

Nazli A, Yang P-C, Jury J, Howe K, Watson JL, Soderholm JD, Sherman PM, Perdue MH and McKay DM (2004) Epithelia under metabolic stress perceive commensal bacteria as a threat. *Am J Pathol* **164**:947-957.

Neal MD, Leaphart C, Levy R, Prince J, Billiar TR, Watkins S, Li J, Cetin S, Ford H, Schreiber A and Hackam DJ (2006) Enterocyte TLR4 mediates phagocytosis and translocation of bacteria across the intestinal barrier. *J Immunol* **176**:3070-3079.

Paiboonsukwong K, Choi I, Matsushima T, Abe Y, Nishimura J, Winichagoon P, Fucharoen S, Nawata H and Muta K (2003) The signalling pathways of erythropoietin and interferon-γ differ in preventing the apoptosis of mature erythroid progenitor cells. *Int J Hematol* **78**:421-428.

Philpott DJ, McKay DM, Sherman PM and Perdue MH (1996) Infection of T84 cells with enteropathogenic *Escherichia coli* alters barrier and transport functions. *Am J Physiol Gastrointest Liver Physiol* **270**:G634-G645.

Prasad S, Mingrino R, Kaukinen K, Hayes KL, Powell RM, MacDonald TT and Collins JE (2005) Inflammatory processes have differential effects on claudins 2, 3 and 4 in colonic epithelial cells. *Lab Invest*. **85**:1139-1162

Satake M, Watanabe H, Miyamoto Y and Shimizu M (2001) Induction of nitric oxide synthase and subsequent production of nitric oxide not involved in interferon-γ-induced hyperpermeability of Caco-2 intestinal epithelial monolayers. *Biosci Biotechnol Biochem* **65**:428-430.

Söderholm JD, Olaison G, Peterson KH, Franzen LE, Lindmark T, Wiren M, Tagesson C and Sjodahl R (2002) Augmented increase in tight junction permeability by luminal stimuli in the non-inflamed ileum of Crohn's disease. *Gut* **50**:307-313.

Song JC, Hanson CM, Tsai V, Farokhzad OC, Lotz M and Matthews JB (2001) Regulation of epithelial transport and barrier function by distinct protein kinase C isoforms. *Am J Physiol Cell Physiol* **281**:C649-C661.

Tomson FL, Koutsouris A, Viswanathan VK, Turner JR, Savkovic SD and Hecht G (2004) Differing roles of protein kinase C-ζ in disruption of tight junction barrier by enteropathogenic and enterohemorrhagic *Escherichia coli*. *Gastroenterology* **127**:859-869.

Unno N, Menconi MJ, Smith M, Aguirre DE and Fink MP (1997) Hyperpermeability of intestinal epithelial monolayers is induced by NO: effect of low extracellular pH. *Am J Physiol Gastrointest Liver Physiol* **272**:G923-G934.

Utech M, Ivanov AI, Samarin SN, Bruewer M, Turner JR, Mrsny RJ, Parkos CA and Nusrat A (2005) Mechanism of IFN-γ-induced endocytosis of tight junction proteins: myosin II-dependent vacuolarization of the apical plasma membrane. *Mol Biol Cell* **16**:5040-5052.

Wang F, Graham WV, Wang Y, Witkowski ED, Schwarz BT and Turner JR (2005) Interferon-γ and tumor necrosis factor-α synergize to induce intestinal epithelial barrier dysfunction by up-regulating myosin light chain kinase expression. *Am J Pathol* **166**:409-419.

Watson JL, Ansari S, Cameron H, Wang A, Akhtar M and McKay DM (2004) Green tea polyphenol (-)-epigallocatechin gallate blocks epithelial barrier dysfunction provoked by IFN-γ but not by IL-4. *Am J Physiol Gastrointest Liver Physiol* **287**:G954-G961.

Weiler F, Marbe T, Scheppach W and Schauber J (2005) Influence of protein kinase C on transcription of the tight junction elements ZO-1 and occludin. *J Cell Physiol* **204**:83-86.

Yang H, Kiristioglu I, Fan Y, Forbush B, Bishop DK, Antony PA, Zhou H and Teitelbaum DH (2002) Interferon-γ expression by intraepithelial lymphocytes results in a loss of epithelial barrier function in a mouse model of total parenteral nutrition. *Ann Surg* **236**:226-234.

Youakim A and Ahdieh M (1999) Interferon-γ decreases barrier function in T84 cells by reducing ZO-1 levels and disrupting apical actin. *Am J Physiol Gastrointest Liver Physiol* **276**:G1279-G1288.

FOOTNOTES

a) This work was supported by a grant from the Canadian Institutes of Health Research (CIHR) to DMM (MT-13421). DMM holds a Canada Research Chair (Tier 1) in Intestinal Immunophysiology in Health and Disease and is an Alberta Heritage Foundation for Medical Research (AHFMR) scientist. JLW was a recipient of a CIHR studentship.

b) Address reprint requests to: Dr. Derek M. McKay, Gastrointestinal Research Group, Department of Physiology and Biophysics, 1877 HS, University of Calgary, 3330 Hospital Drive NW, Calgary, Alberta, Canada T2N 4N1 Tel: (403) 220-7362 Fax: (403) 210-8999 email: dmckay@ucalgary.ca

Legends for Figures

Figure 1: PI-3K activity is necessary for IFNγ-induced increases in epithelial permeability. T84 epithelial monolayers were grown on filter supports and treated with IFNγ (20ng/ml) ± LY294002 (LY; n = 6-30 monolayers per condition (panel A)) or wortmannin (W; n = 4-6 monolayers per condition (panel B)) and transepithelial electrical resistance (TER) assessed 48h later. Co-treatment with LY (20μM) inhibits the increases in transepithelial flux of ^{51}Cr-EDTA (n = 9 monolayers per condition (panel C)) and horseradish peroxidase (HRP; n = 6 monolayers per condition (panel D)) observed 48h after IFNγ treatment (data are mean ± SEM; *, $p<0.05$ compared to control (CON); #, $p<0.05$ compared to LY at 5 and 20 μM; starting TER range = 1410-3560 Ω/cm^2).

Figure 2: A phosphatidylinositiol analogue (PIA) inhibits IFNγ-induced decreases in transepithelial electrical resistance (TER). Assessment of TER 48h after exposure to PIA revealed no change compared to pre-treatment values, whereas the drop in TER observed 48h after treatment with IFNγ (20ng/ml) was blocked by PIA (data are mean ± SEM; *, $p<0.05$ compared to control (CON); n = 6 monolayers per condition; starting TER range = 1120-2340 Ω/cm^2).

Figure 3: Pharmacological blockade of PI-3K activity 6h after IFNγ exposure is sufficient to prevent the reduced transepithelial electrical resistance (TER). T84 epithelial monolayers were treated with IFNγ (20ng/ml) followed by LY294002 (LY: 20μM) simultaneously (i.e. 0h) or 3, 6, 12, and 24h post-IFNγ addition, and TER assessed 48h after the IFNγ addition (data are mean ±

SEM; *, $p<0.05$ compared to control (CON); n = 4-8 monolayers per condition; starting TER range = 1470-2440 Ω/cm^2).

Figure 4: Epithelial barrier dysfunction induced by enteropathogenic *Escherichia coli* (EPEC) is not mediated by PI-3K inhibition. EPEC ($5x10^7$ cfu) ± LY294002 (LY: 20μM) were added to the apical and basolateral side of confluent T84 epithelial monolayers, respectively, and transepithelial electrical resistance (TER) assessed 24h later (data are mean ± SEM; n = 8 monolayers per condition; *, $p<0.05$ compared to control; starting TER range = 1580-2460 Ω/cm^2).

Figure 5: Inhibition of constitutive or inducible nitric oxide synthases (NOS) does not ameliorate IFNγ-induced deceases in transepithelial electrical resistance (TER). Pre-treatment of T84 epithelial monolayers with inhibitors of NOS, L-NAME (1mM), L-NMMA (100μM) and L-NIL (10μM) did not prevent the drop in TER evoked by IFNγ (20ng/ml; 48h) (data are mean ± SEM; n = 6-12 monolayers per condition; *, $p<0.05$ compared to control (CON); starting TER range = 1450-2950 Ω/cm^2). Inset, IFNγ treatment (20 ng/ml, 6h) results in a subtle increase in cNOS and an obvious up-regulation of iNOS mRNA expression (3 separate epithelial preparations are shown per treatment and the bands depicted are of the predicted size based on primer sequence design).

Figure 6: Inhibition of PI-3K does not affect IFNγ-induced STAT1 DNA binding activity or induced IRF-1 expression. A) Nuclear protein extracts from T84 epithelial monolayers treated with IFNγ (20ng/ml, 30 min) displayed obvious STAT1 DNA binding on EMSA, that was not

affected by pre-treatment with LY294002 (LY; 20μM) or wortmannin (W; 0.1μM) but was reduced by aurintricarboxylic acid (ATA; 50 μM) and (-)-epigallacatechin gallate (EGCG; 100μM) (n = 3). B) Under the same experimental conditions a small increase in STAT1 ^{727}serine phosphorylation was induced by IFNγ that was unaffected by LY pretreatment (n=3). C) IFNγ-evoked increased protein expression of interferon-regulated factor (IRF)-1 was not affected by either LY or wortmannin, but was reduced by EGCG treatment as determined by immunoblotting of whole cell protein extracts (n = 2: actin is included as a protein loading control).

Figure 7: AKT is not involved in IFNγ-induced decreases in transepithelial electrical resistance (TER). Panel A shows that use of either inhibitors of AKT activity, SH-5 or API-2 (20μM) (n=8-12 epithelial monolayers per condition) failed to ameliorate the drop in TER observed 48h post-IFNγ treatment (20ng/ml). Panel B is a representative immunoblot of whole cell protein extracts (n=4), showing that while insulin-like growth factor (IGF)-1 (10ng/ml, 15 min) results in increased phosphorylation of AKT ^{473}serine (p-AKT) in T84 cells, there was no consistent induction of AKT activation by IFNγ even with 10-fold more cytokine (i.e. 200ng/ml) than that required to cause increased epithelial permeability.

Figure 8: Inhibition of PKC activity reduces the IFNγ-induced decrease in transepithelial resistance (TER). Panel A shows that a 45 min pre-treatment with the general PKC inhibitor bisindolylmalemide I (BIM; 5μM) significantly reduced the drop in TER caused by IFNγ (20ng/ml; 48h) (data are mean ± SEM; #, p = 0.004 compared to IFNγ using Students paired t-test (n=19 experiments, 2-3 epithelial monolayers per experiment)). In the same

experiments PI-3K inhibition by LY294002 (LY; 20μM) completed prevented the effect of IFNγ (n = 13). Panel B shows when added 6h after IFNγ, bis. was equally effective in blocking the drop in TER as compared to BIM pre-treatment (each symbol indicates a separate experiment and is the mean value of 2-3 epithelial monolayers per experiment) ((solid line is the arithmetic mean; *, $p<0.05$ compared to control via ANOVA; starting TER range = 940-3280 Ω/cm^2).

Figure 9: Bar graph showing total preservation of epithelial barrier function (assessed by transepithelial electrical resistance (TER)) in IFNγ (20 ng/ml; 48h) exposed T84 cell monolayers co-treated with the PI-3K inhibitor, LY294002 (LY; 20 μM) ± the general PKC inhibitor, bisindolylmalemide I (BIM; 5μM) (data are mean ± SEM; n = 5 experiments with 9-16 epithelial monolayers/condition; starting TER range = 1000-2250Ω/cm^2; * and #, $p<0.05$ compared to control and IFNγ only)

Figure 10: PI-3K inhibition inhibits IFNγ-induced increased in internalization and transcytosis of non-invasive *E. coli* HB101 across T84 epithelial monolayers. (A) Representative images taken 16h after *E. coli* HB101 inoculation showing extracellular (yellow/orange) and intracellular (green) bacteria under the denoted experimental conditions (IFNγ, 20 ng/ml, 48h ± the PI-3K inhibitor, LY294002 (LY: 20 μM) (phase contrast and fluorescence microscopy overlay. White line demarcates the edge of the epithelium)). Treatment with IFNγ results in greater bacterial internalization (enhanced green in the image (centre panel)). (B) A representative experiment showing control monolayers (n = 6; i.e. each division on the agar plate) or cells treated with IFNγ ± LY for 48h at which time *E. coli* (10^6 cfu) was added to the apical aspect of the monolayers and basolateral medium collected 16h later and grown overnight

on LB agar plates (numbers represent the assigned score for each bacterial translocation; Ψ, contamination). Panel C shows the quantification of the translocation studies, where inhibition of PI-3K (with LY) and PKC (with bisindolylmalemide I (BIM; 5 μM)) was found to significantly inhibit IFNγ enhancement of *E. coli* translocation ((data are mean ± SEM; n = number of epithelial monolayers; *, $p<0.05$ compared to control (CON); ‡, $p<0.05$ compared to IFNγ only). Panel D summarizes the percentage of bacterial translocations scored as 5 (i.e. uncountable colonies growing as a bacterial lawn) from each of the conditions shown in panel C.

Figure 11: Panel A) shows the quantification of *E.coli* HB101 translocation across T84 epithelial monolayers 48h after exposure to IFNγ (20 ng/ml) ± co-treatment with the PI-3K inhibitor, LY294002 (LY; 20 μM), the PKC inhibitor, bisindolylmalemide I (BIM; 5 μM)) or both drugs (data are mean ± SEM of 4 separate (numbers inside the bars indicate the number of epithelial monolayers/condition); *, $p<0.05$ compared to control; †, $p<0.05$ compared to IFNγ only). Panel B summarizes the percentage of bacterial translocations scored as 5 (i.e. uncountable colonies growing as a bacterial lawn) from each of the conditions shown in panel A).

Figure 12: Diagrammatic hypothetical schema of the intracellular signalling pathways mobilized in epithelial cells in response to IFNγ that affect epithelial paracellular and transcellular permeability. In response to IFNγ, PI-3K is activated, and in the absence of detectable Akt activation, protein kinase C (PKC) is mobilized via either PDK1 or an intermediate molecule. PI-3K either directly and/or via PKC, and possibly other unidentified intermediates, regulates the transcription and translation of tight junction (TJ) proteins, or regulators thereof, and/or affects the trafficking and insertion of TJ proteins into the junction complex. Simultaneously PI-3K and PKC activation allow for enhanced entry of non-invasive bacteria into the enterocyte and

transcytosis across the cell. STAT1 is activated in response to IFNγ, and while capable of leading to increased nitric oxide (NO), NO appears not to be involved in the increased paracellular permeability in this model system (CHX, cyclohexamide; IFNGR, IFNγ receptor; iNOS, inducible nitric oxide synthase; ●, phosphorylation).

Tables

Table 1: *Inhibition of PKC pathways does not affect IL-4 induced reductions in T84 monolayer transepithelial electrical resistance (TER)*

Condition	% pre-treatment TER	n
Control (medium only)	86 ± 2	18
Bisindolylmalemide I (BIM)	94 ± 1	12
IL-4 (10 ng/ml; 24h)	56 ± 6*	18
BIM (200 nM) + IL-4	58 ± 4*	12
BIM (5 μM) + IL-4	38 ± 1#	6

(Confluent monolayers were pre-treated with the PKC inhibitor, BIM. for 8h. IL-4 and fresh BIM were then added to the basal compartment of the culture well and TER assessed 24h later; data are mean ± SEM; n=epithelial monolayers; *, $p<0.05$ compared to control and #, $p<0.05$ compared to control and IL-4 treatment)

Table 2: *Inhibition of PI-3K prevents IFNγ-induced E. coli internalization*

	Conditions		
Exp. #	Control	IFNγ	IFNγ + LY
1	1780	3200	450
2	744	1678	107
3	2800	5511	3067
4	66	587	33

One million T84 epithelial cells were seeded into Petri dishes and 3-4 days later were treated with 20ng/ml IFNγ ± LY294002 (LY: 20μM) for 48h. The medium was replaced with fresh antibiotic-free medium containing 10^6 cfu *E. coli* HB101. Sixteen hours later extracellular bacteria were killed by gentamicin treatment, followed by epithelial lysis and enumeration of internalized bacteria (mean colony counts from 4 experiments, 2-3 epithelial preparations per condition per experiment).

JPET Fast Forward. Published on December 18, 2006 as DOI: 10.1124/jpet.106.113639
This article has not been copyedited and formatted. The final version may differ from this version.

McKay *et al*., 2006 Figure 1 A & B

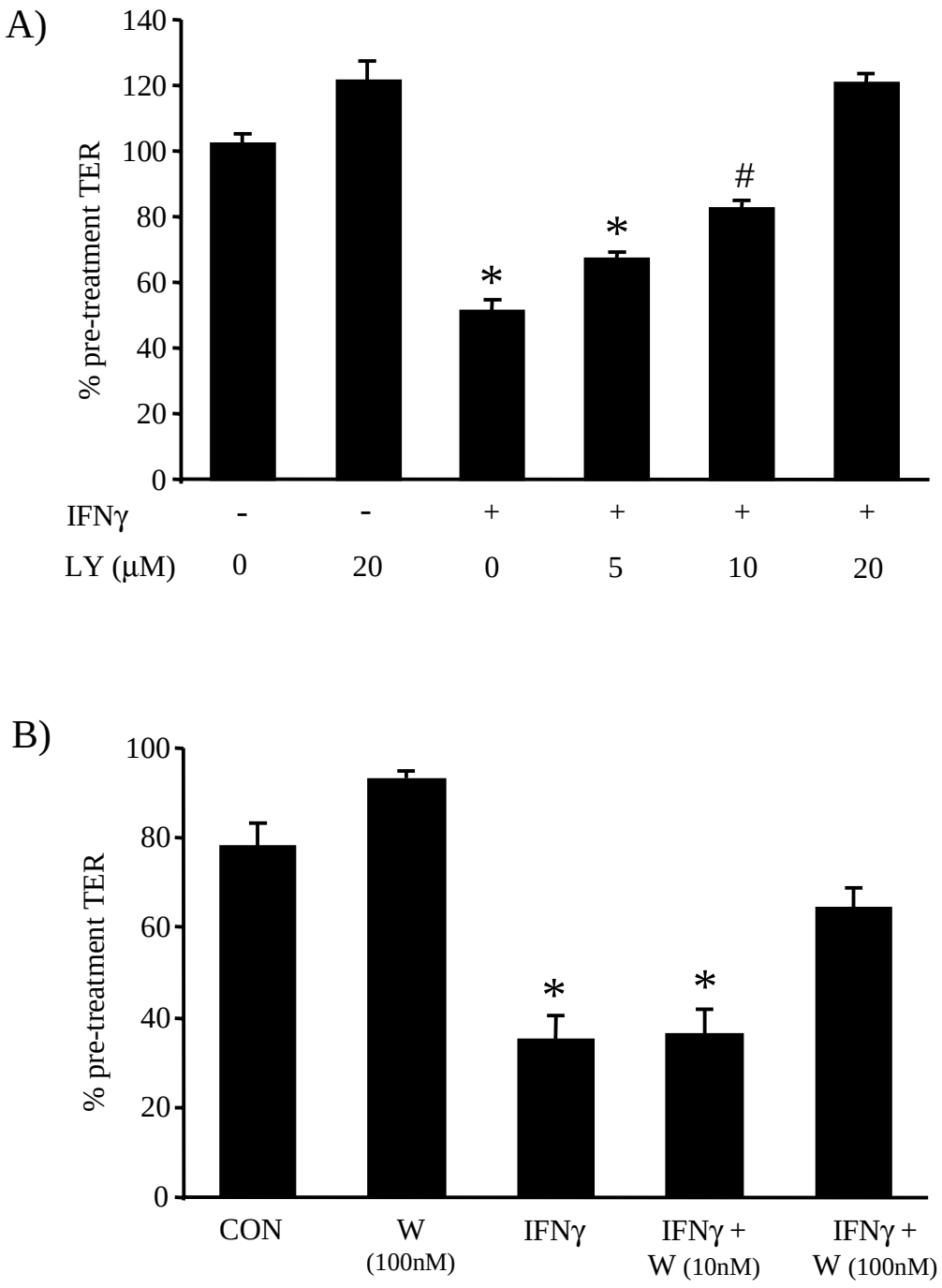

JPET Fast Forward. Published on December 18, 2006 as DOI: 10.1124/jpet.106.113639
This article has not been copyedited and formatted. The final version may differ from this version.

McKay *et al*., 2006 Figure 1 C & D

C)

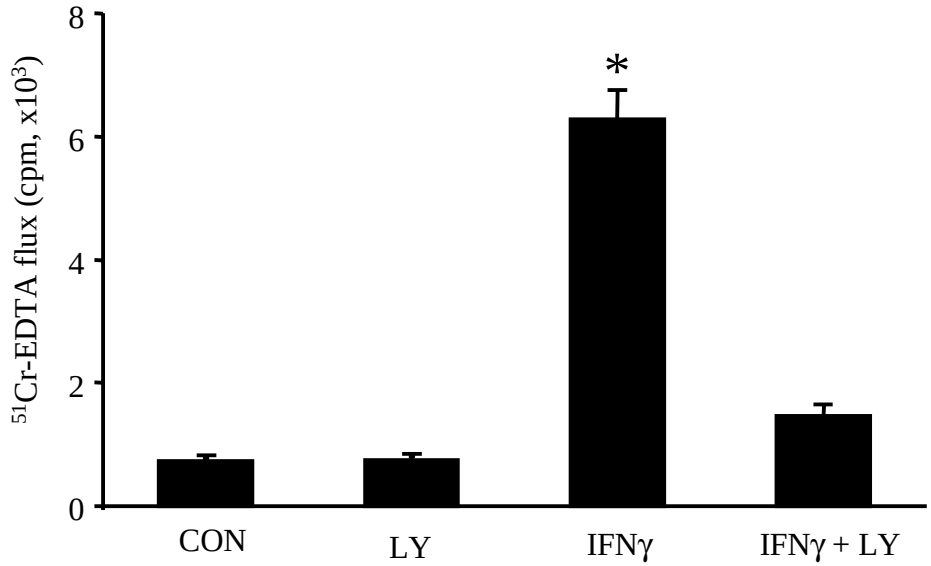

D)

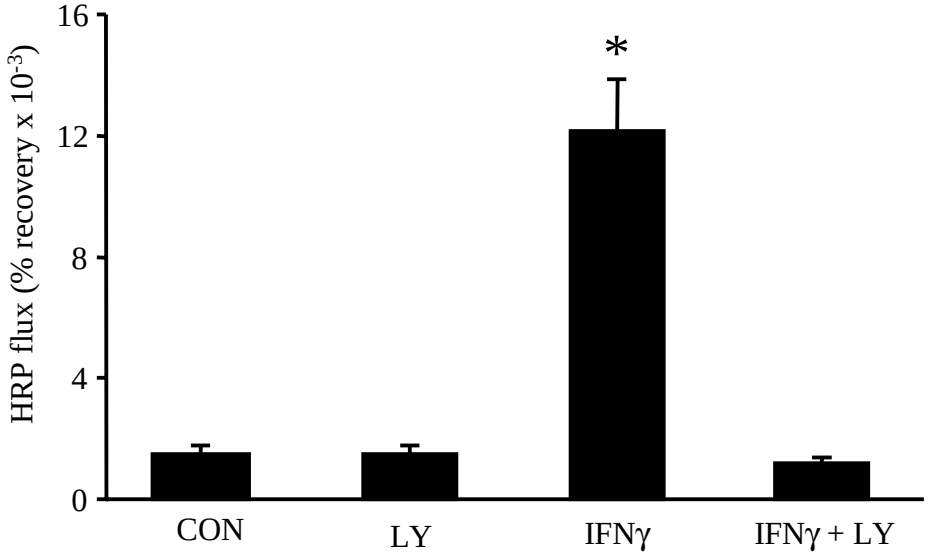

JPET Fast Forward. Published on December 18, 2006 as DOI: 10.1124/jpet.106.113639
This article has not been copyedited and formatted. The final version may differ from this version.

McKay *et al*., 2006 Figure 2

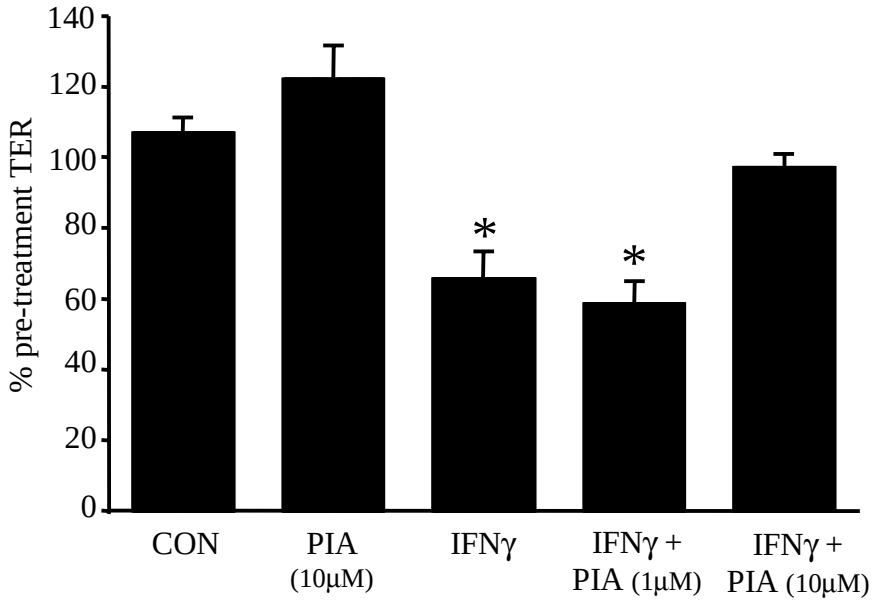

JPET Fast Forward. Published on December 18, 2006 as DOI: 10.1124/jpet.106.113639
This article has not been copyedited and formatted. The final version may differ from this version.

McKay *et al*., 2006 Figure 3

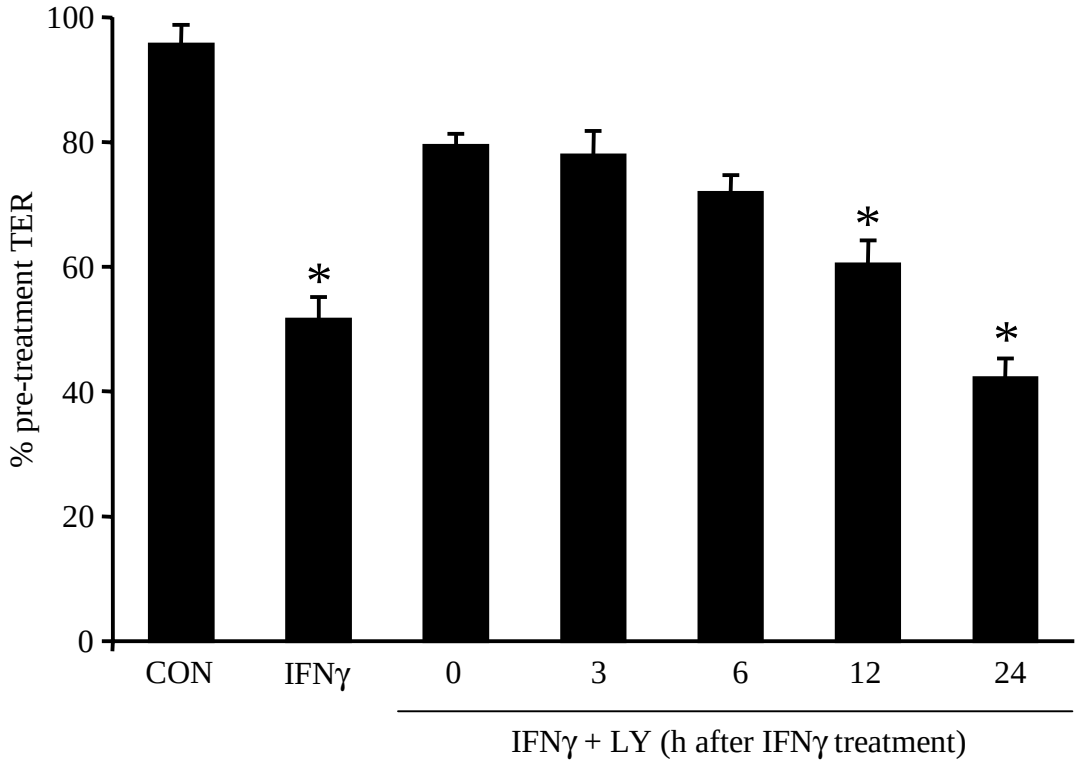

JPET Fast Forward. Published on December 18, 2006 as DOI: 10.1124/jpet.106.113639
This article has not been copyedited and formatted. The final version may differ from this version.

McKay *et al*., 2006 Figure 4

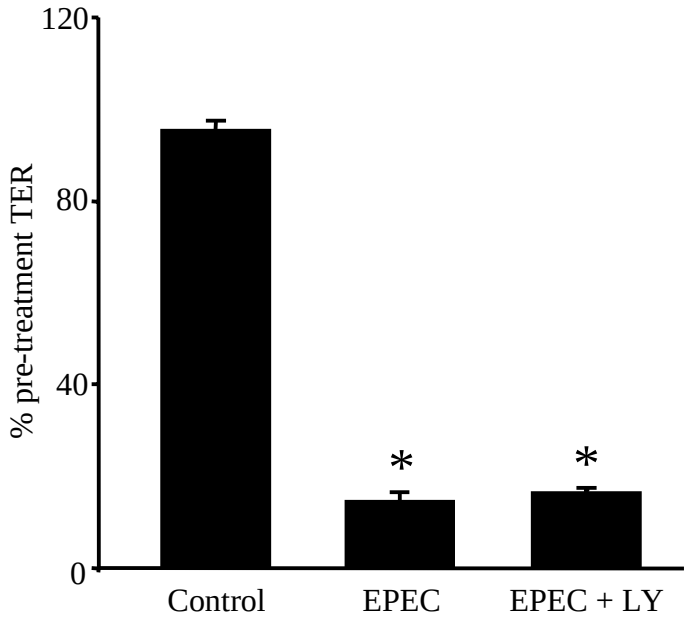

JPET Fast Forward. Published on December 18, 2006 as DOI: 10.1124/jpet.106.113639
This article has not been copyedited and formatted. The final version may differ from this version.

McKay *et al*., 2006 Figure 5

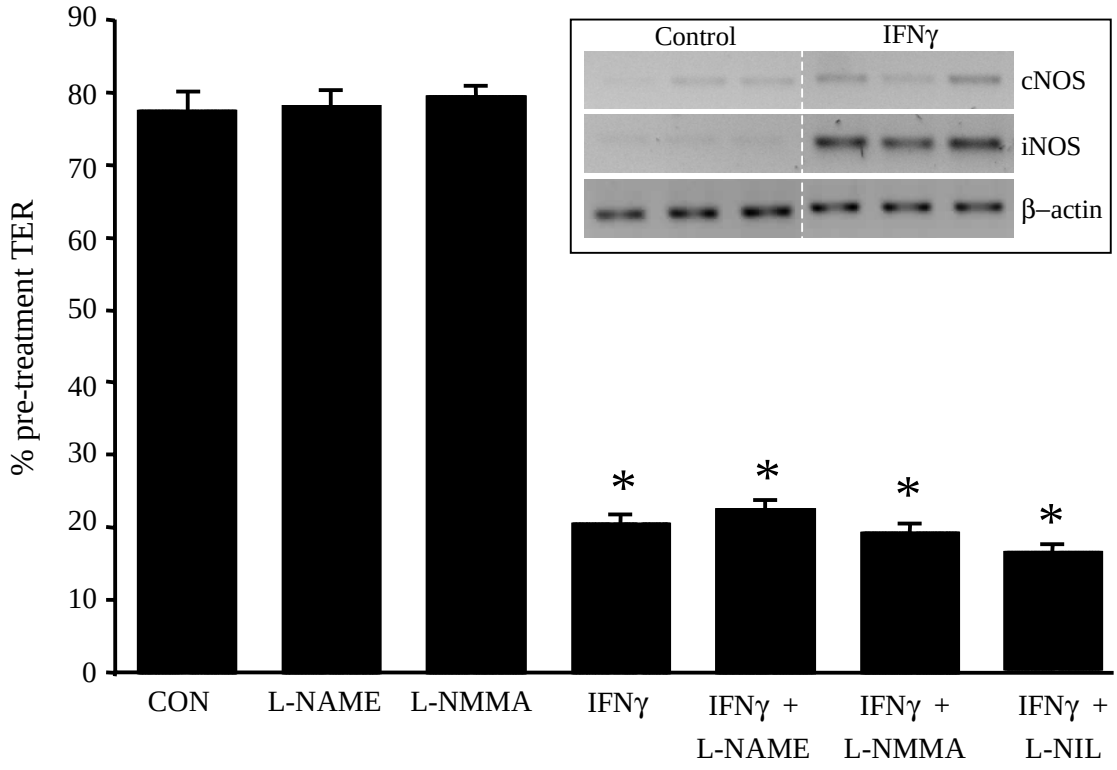

JPET Fast Forward. Published on December 18, 2006 as DOI: 10.1124/jpet.106.113639
This article has not been copyedited and formatted. The final version may differ from this version.

McKay *et al*., 2006 Figure 6A-C

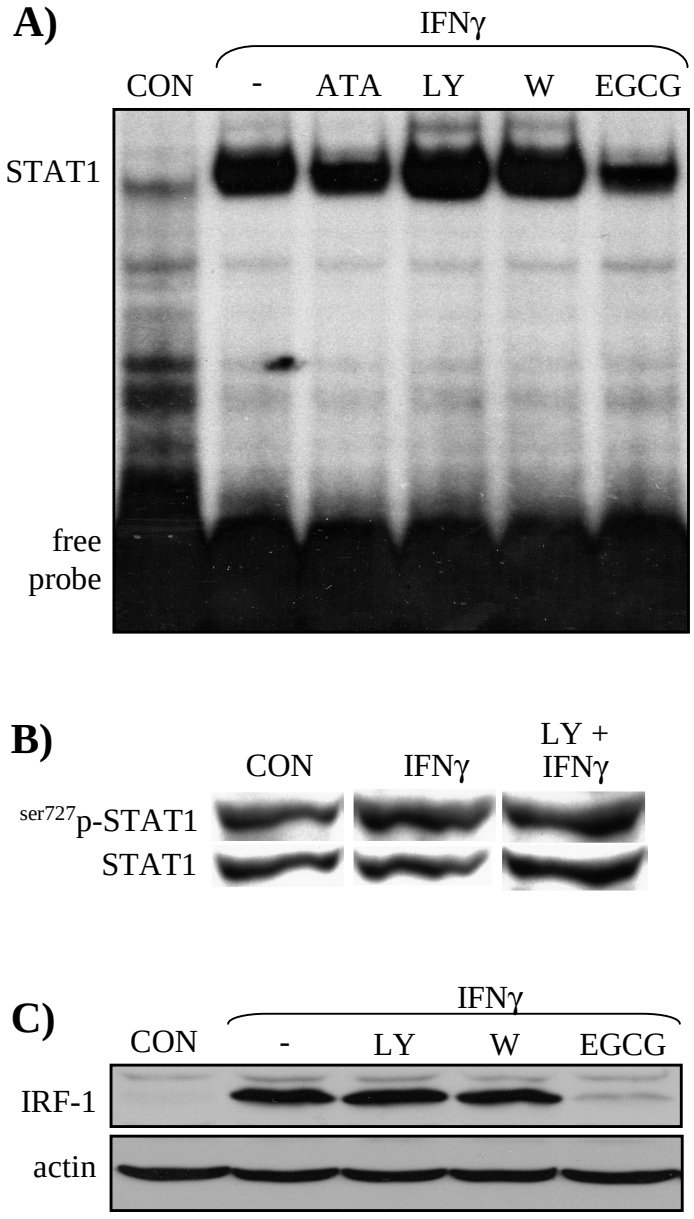

JPET Fast Forward. Published on December 18, 2006 as DOI: 10.1124/jpet.106.113639
This article has not been copyedited and formatted. The final version may differ from this version.

McKay *et al*., 2006 Figure 7A & B

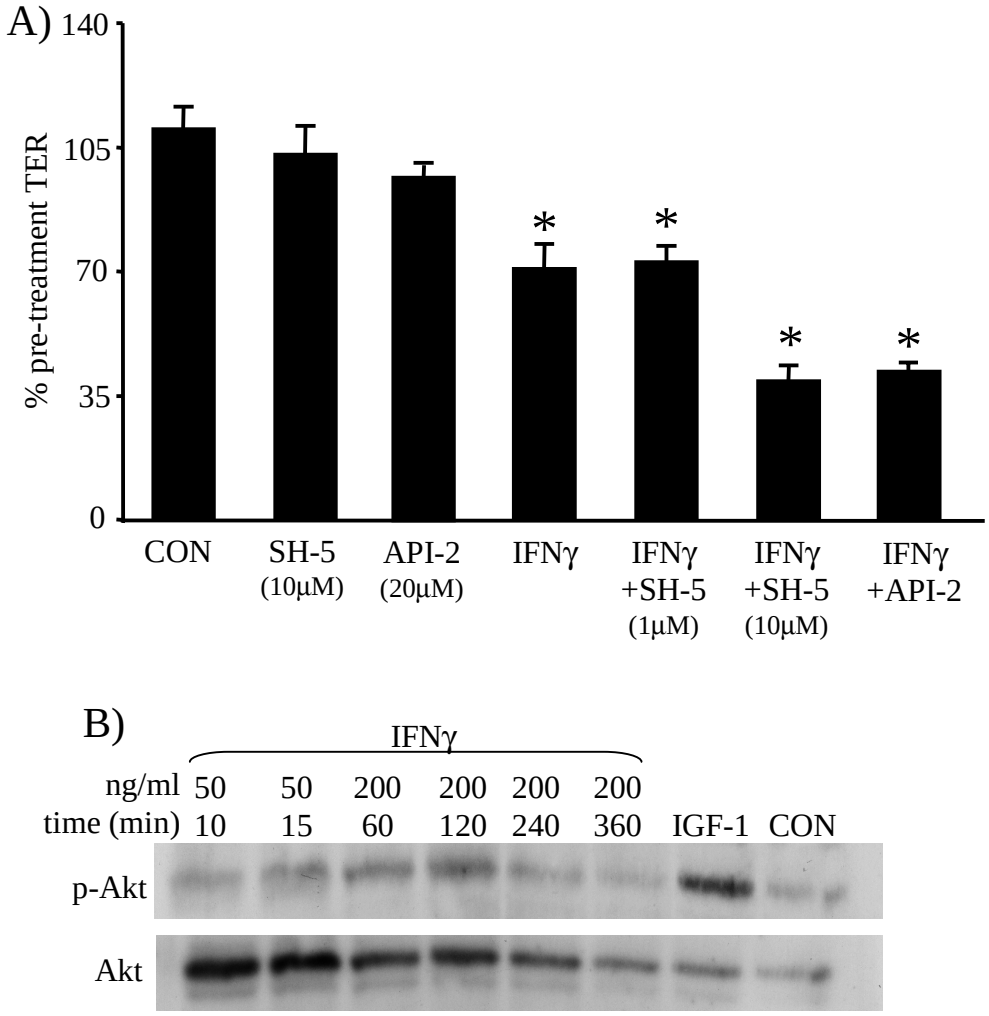

JPET Fast Forward. Published on December 18, 2006 as DOI: 10.1124/jpet.106.113639
This article has not been copyedited and formatted. The final version may differ from this version.

McKay *et al*., 2006 Figure 8A & B

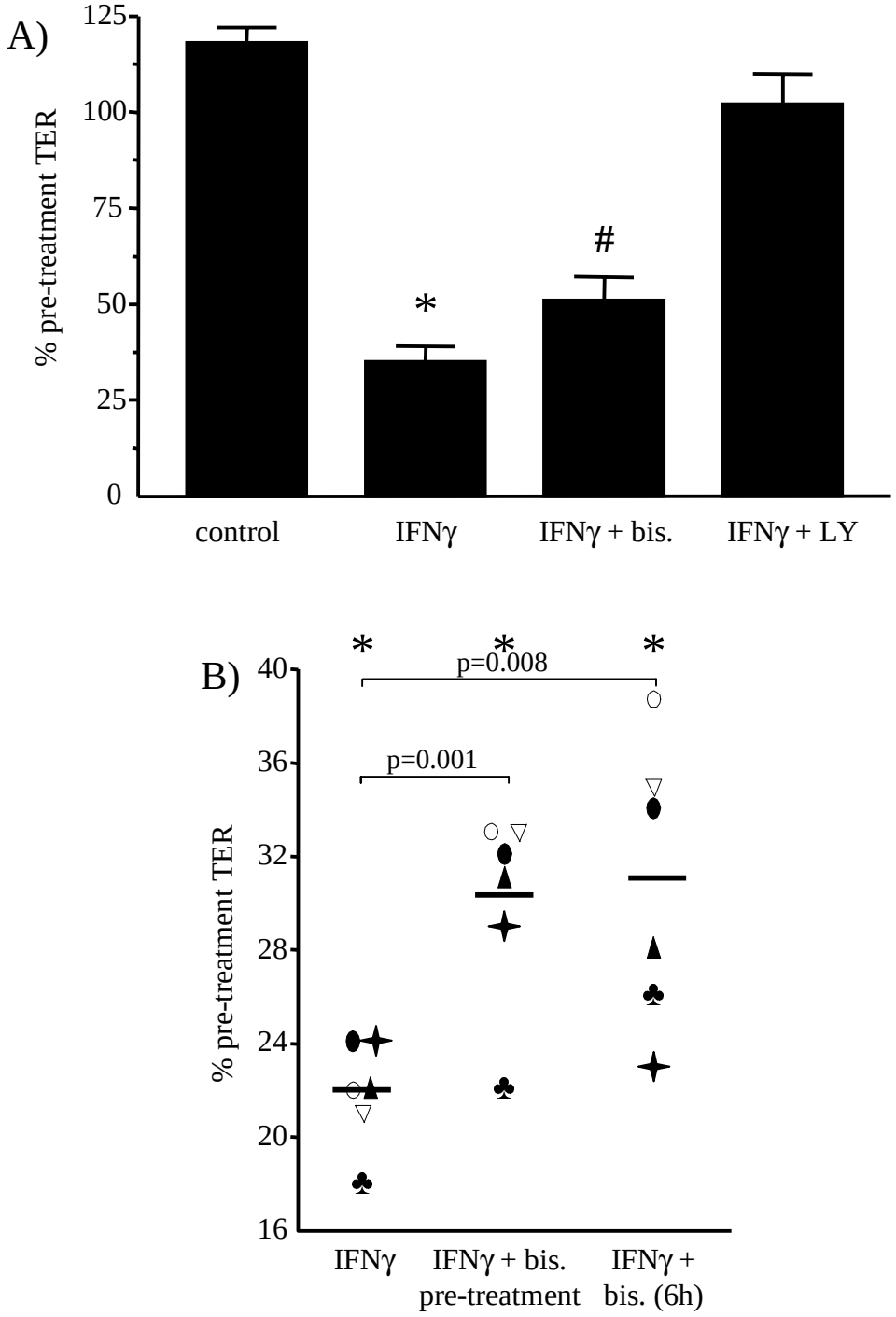

JPET Fast Forward. Published on December 18, 2006 as DOI: 10.1124/jpet.106.113639
This article has not been copyedited and formatted. The final version may differ from this version.

McKay *et al*., 2006 Figure 9

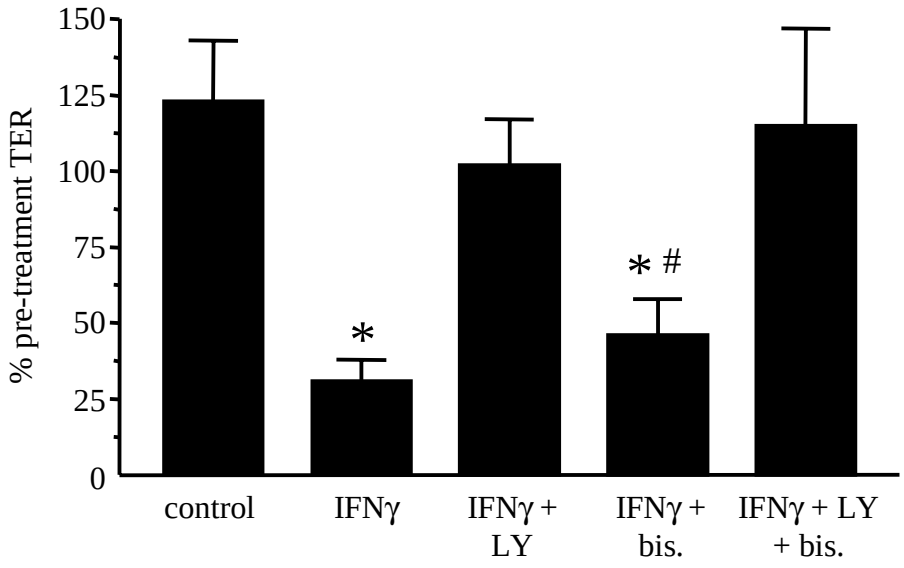

JPET Fast Forward. Published on December 18, 2006 as DOI: 10.1124/jpet.106.113639
This article has not been copyedited and formatted. The final version may differ from this version.

McKay *et al*., 2006 Figure 10 A-D

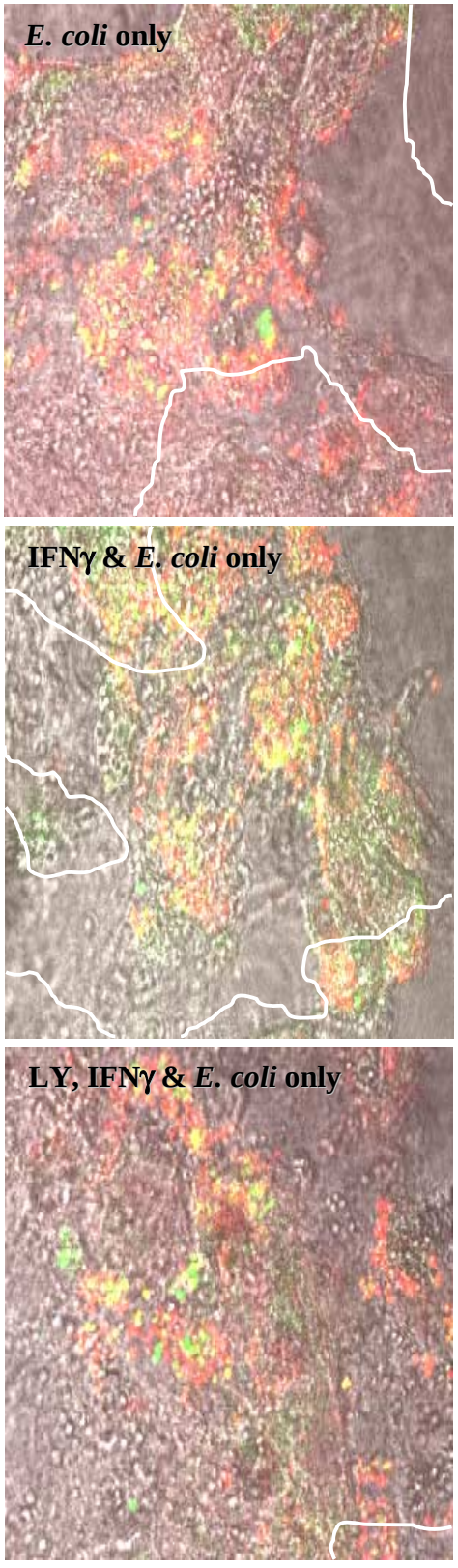

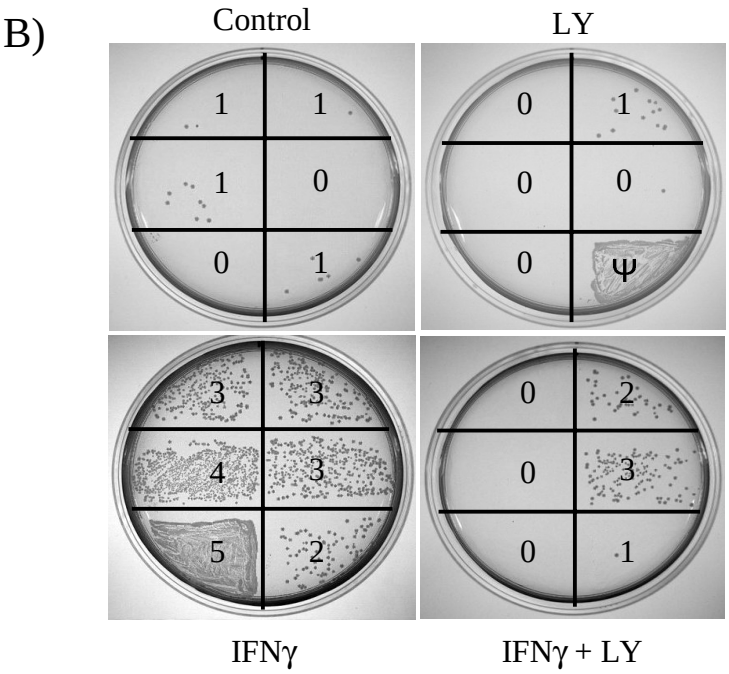

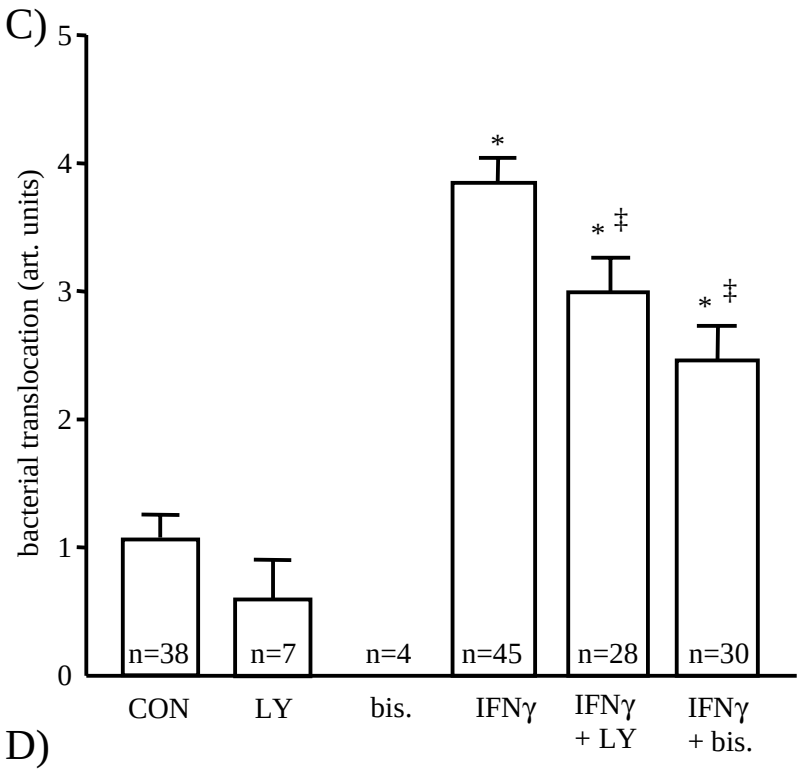

D)

% preps. graded as 5	0	0	0	44	26	0

JPET Fast Forward. Published on December 18, 2006 as DOI: 10.1124/jpet.106.113639
This article has not been copyedited and formatted. The final version may differ from this version.

McKay *et al*., 2006 Figure 11

A)

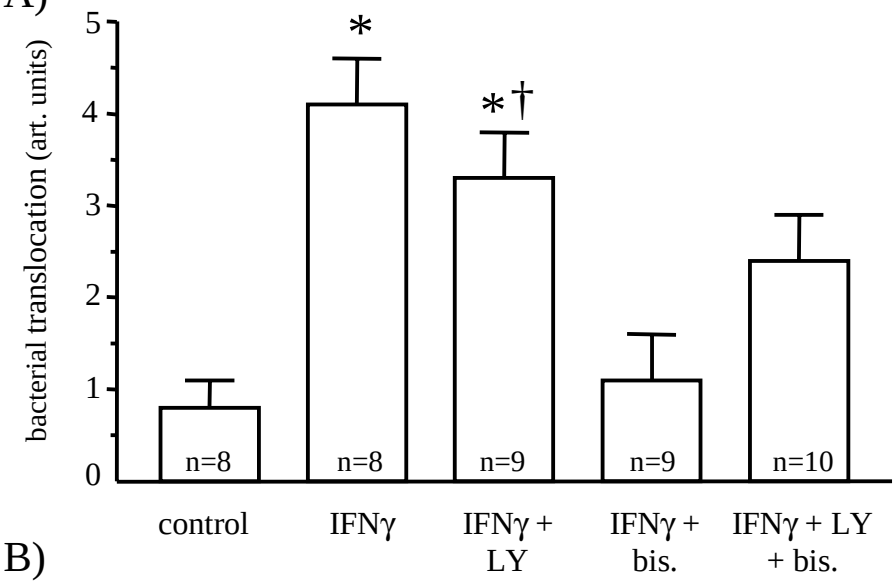

B)

% preps. graded as 5	0	50	33	0	10

JPET Fast Forward. Published on December 18, 2006 as DOI: 10.1124/jpet.106.113639
This article has not been copyedited and formatted. The final version may differ from this version.

McKay *et al*., 2006 Figure 12